Journal Pre-proofs

Facile modification of protein-imprinted polydopamine coatings over nanoparticles with enhanced binding selectivity

Wenyan Han, Xiao Han, Zhiqiang Liu, Shiting Zhang, Yang Li, Jinyan Lu, Jian Chen, Lailiang Ou, Guoqi Fu

PII: S1385-8947(19)32876-1
DOI: https://doi.org/10.1016/j.cej.2019.123463
Reference: CEJ 123463

To appear in: *Chemical Engineering Journal*

Received Date: 4 July 2019
Revised Date: 5 November 2019
Accepted Date: 11 November 2019

Please cite this article as: W. Han, X. Han, Z. Liu, S. Zhang, Y. Li, J. Lu, J. Chen, L. Ou, G. Fu, Facile modification of protein-imprinted polydopamine coatings over nanoparticles with enhanced binding selectivity, *Chemical Engineering Journal* (2019), doi: https://doi.org/10.1016/j.cej.2019.123463

Facile modification of protein-imprinted polydopamine coatings over nanoparticles with enhanced binding selectivity

Wenyan Han[a], Xiao Han[b], Zhiqiang Liu[b], Shiting Zhang[b], Yang Li[c], Jinyan Lu[a], Jian Chen[a], Lailiang Ou*[,a], Guoqi Fu*[,b]

[a] Key Laboratory of Bioactive Materials of Ministry of Education , College of Life Science, Nankai University, Tianjin 300071, China

[b] Key Laboratory of Functional Polymer Materials of Ministry of Education, Institute of Polymer Chemistry, College of Chemistry, Nankai University, Tianjin 300071, China

[c] College of Pharmacy, Nankai University, 38 Tongyan Road, Tianjin 300071, China

* Corresponding author.

E-mail address: ouyll@nankai.edu.cn (L. Ou); gqfu@nankai.edu.cn (G. Fu)

Tel: 86 22 23501443

Abstract:

Mussel-inspired dopamine (DA) self-polymerization over a variety of substrates has become a simple but versatile approach for synthesis of surface protein-imprinted materials. However, relatively high nonspecific binding to the imprinted polydopamine (PDA) coatings has long been an open problem because of their multifunctionalities. We herein propose a facile strategy for reduction of the nonspecific adsorption by covering the imprinted PDA coatings with slightly crosslinked nonlinear poly(ethylene glycol) (PEG) layers via aqueous precipitation polymerization before template removal. Vinyl groups are introduced onto the PDA coatings via Cu^{2+} mediated metal coordination for facilitating surface polymerization. The Cu^{2+} and embedded template are removed after polymerization. For proof of hypothesis, the protein imprinted PDA coatings were formed with SiO_2 nanoparticles as representative nano-supports and lysozyme as a model protein template. Protein binding tests show that the grafted PEG layers with an optimized feed crosslinking degree can significantly enhance both recognition selectivity and specific binding capacity to the imprinted nanoparticles, typically with the imprinting factor increasing from 2.6 to 6.4. Also, the PEG layers can remarkably improve the stability of the PDA coatings in the acidic template removal solution. The presented strategy represents the first example for PEGylation of protein-imprinted PDA coatings, and may be extended for surface imprinting of other bio/organic molecules over other substrate materials.

Keywords: protein imprinting; molecular imprinting; polyopamine; mussel-inspired coatings; aqueous precipitation polymerization; nanoparticles.

1. Introduction

Molecularly imprinted polymers (MIPs) are tailor-made materials mimicking the recognition of biological receptors. MIPs are generally synthesized by copolymerizing suitable functional and cross-linking monomers in the presence of desired template molecules, and upon subsequent template removal, the polymer is left with target recognition cavities (imprinting sites) complementary to the template molecules in shape, size and functional groups. They outperform these natural receptors due to their high stability, ease of obtention and low cost [1]. Till now, the imprinting of proteins and other biomacromolecules is still challenged due to their large size, complex structure, variable conformation, and significantly reduced template-monomer interactions in the required aqueous polymerization media [2-4]. For overcoming these limitations, a diversity of strategies have been proposed, such as epitope imprinting [5], surface imprinting [6-13], and nanoscale imprinting [14-16]. The combination of latter two methods, i.e. surface imprinting over nanostructures [17], has proved to be an effective solution to both alleviate the biomacromolecular transfer difficulty and achieve high binding capacity. Furthermore, the imprinting performance of the final imprinted nanocomposites can be enhanced by appropriate surface functionalization of the nanosized substrates [8,9].

The adhesive proteins of mussels contain extremely high concentrations of catechol and amine functional groups, and are capable of mediating adhesion to multifarious surfaces. Lee et al. [18] found that dopamine (DA), commonly known as a neurotransmitter, is also a small-molecule mimic of the adhesive proteins. They hence reported a simple but versatile surface modification approach in which self-polymerization of DA at weak alkaline pH and

room temperature produced an adherent polydopamine (PDA) coating on a wide variety of organic and inorganic materials. On the other hand, DA can interact with protein molecules via multiple forces such as hydrogen bonding, electrostatic attraction and π-π stacking [19-22]. Therefore, the mussel-inspired PDA coating has become one of the most important approaches for surface protein imprinting over different nanomaterials and other substrates, such as SiO_2 nanoparticles [23], Fe_3O_4 nanoparticles [24-26], Fe_3O_4@SiO_2 nanoparticles [27-30], quantum dots [31], silicon wires [32], carbon nanotubes [33], graphene [34], flat gold chips [35,36], and porous polymer monolith [37]. More than 100 studies about protein-imprinted PDA coatings have been published since Lee et al.'s work [18] in 2007. These studies aimed at a wide range of applications, such as separation (depletion or enrichment) of target proteins in biosamples [23,25,26,33,34,37], biosensing [35,36], and artificial enzyme inhibitors [27,33].

PDA coatings are featured with plenty of multiple functional groups, such as amine, indole, catechol and quinone groups [38-40]. This is advantageous to the formation of high-affinity cavities within the protein-imprinted PDA coatings, but these groups left in the non-cavity regions, especially on the surface, can lead to significant nonspecific adsorption. However, this problem has been rarely addressed, probably since that, unlike the protein imprinting based on copolymerization of several kinds of (meth)acrylic monomers with tunable compositions, the polymerization solutions containing only DA monomer are difficult to be tuned. The post-imprinting modification strategy may be a rational choice, which is based on surface modification of the noncavity regions of the protein MIPs in the presence of the template with a protein-resistant polymer [41, 42]. Li et al. [41] modified protein-imprinted

PDA-coated magnetic microspheres with an atom transfer radical polymerization (ATRP) initiator and then grafted zwitterionic poly(2-methacryloyloxyethyl phosphorylcholine) (PMPC) chains via surface-initiated ATRP. The grafted PMPC chains could greatly increase protein binding selectivity to the MIP microspheres. To the best of our knowledge, till now this is the only study on increasing the binding selectivity of protein-imprinted PDA coatings via post-imprinting modification. However, the disadvantages of this method include inconvenient ATRP procedures and unfriendly reaction conditions (using CH_2Cl_2 and DMF as the reaction media and performing ATRP at up to 80 °C).

Polyethylene glycol (PEG) is a highly flexible, nonionic, hydrophilic and biocompatible polymer. It is extensively used in biomedical fields as a blocking agent to resist nonspecific adsorption of proteins on implant surfaces and nanoparticles intended for therapy, imaging and biodetection [43,44]. The protein-repelling effect of PEG is attributed to the low free energy at PEG−water interface and the absence of hydrogen bonding and electrostatic interactions with proteins [45]. For the first time, Luan et al. [42] grafted PEG chains from the surface of protein-imprinted siloxane copolymers before template removal by reaction of the surface silanol groups with methoxy-PEG-silane for lowering nonspecific protein adsorption. According to the grafting mechanism, this approach is primarily applicable to PEGylation of the protein MIPs bearing silanol groups fabricated via sol-gel process, and may be not suitable for surface modification of the imprinted PDA coatings without silanol groups.

As a typical nonlinear PEG analogue, poly(di(ethylene glycol) methacrylate) ($PMEO_2MA$) is also featured by its protein-resistance and biocompatibility like the linear PEG. Additionally, it is a thermo-responsive polymer, with a lower critical solution temperature

(LCST) of about 26 °C [46]. Recently, we have synthesized surface protein-imprinted nanoparticles via aqueous precipitation copolymerization of MEO_2MA with other functional monomers, and the resulting imprinted nanoparticles showed relatively low nonspecific binding due to the protein-repelling character of $PMEO_2MA$ [47,48]. Inspired by these studies, herein we propose a facile and green modification approach for enhancement of the binding selectivity of protein-imprinted PDA coatings. This is achieved via surface grafting of slightly crosslinked nonlinear PEG layers by radical-induced aqueous precipitation copolymerization of MEO_2MA with a crosslinker at 37 °C before template removal. Polymerisable vinyl groups are introduced onto the imprinted PDA coatings via metal chelating for facilitating surface polymerization. For proof of this concept, SiO_2 nanoparticles were used as representative nano-substrates and lysozyme (Lyz) as well as bovine hemoglobin (BHb) as model protein templates for fabrication of core-shell protein-imprinted nanoparticles via DA self-polymerization, followed by surface grafting of crosslinked $PMEO_2MA$ layers with an optimized feed crosslinking degree. The effect of grafted $PMEO_2MA$ layers on the protein recognition properties was studied by batch binding experiments and sodium dodecyl sulfate polyacrylamide gel electrophoresis (SDS-PAGE) analysis. The influence of the $PMEO_2MA$ layers was also examined on the stability of the internal protein-imprinted PDA coatings.

2. Materials and methods

2.1 Materials

See Supporting Information.

2.2 Synthesis of Lyz-imprinted nanoparticles via PDA coating over functionalized SiO_2 nanoparticles

Synthesis of carboxyl functionalized SiO_2 nanoparticles (denoted as SiO_2-COOH) is detailed in Supporting Information. For imprinting of Lyz over the SiO_2-COOH nanoparticles via DA self-polymerization, Lyz (40 mg) was dissolved in 40 mL Tris buffer (20 mM, pH 8.0) containing the SiO_2-COOH nanoparticles (200 mg). To this dispersion, DA (80 mg) was added, and then the mixture was stirred with exposure to air at 25 °C for 12 h. The resultant imprinted nanoparticles were collected by centrifugation, washed repeatedly with 1% SDS/3% HAc solution to remove the embedded template until no Lyz in the supernatant was detected using a UV/Vis spectrophotometer at 280 nm, with deionized water and 0.5 M NaCl solution to remove the remaining SDS and HAc, with distillated water to remove the remaining NaCl, and finally freeze-dried to constant weight. The control non-imprinted nanoparticles were prepared and treated in the same way but in absence of the template. The resulting imprinted and non-imprinted nanoparticles were denoted as Lyz-MIP and NIP (non-imprinted polymer), respectively.

2.3 Grafting of crosslinked $PMEO_2MA$ layers from Lyz-imprinted nanoparticles

The Lyz-imprinted as well as the non-imprinted nanoparticles used for grafting of crosslinked $PMEO_2MA$ layers were synthesized in the same way as described above but without removal of the template. Firstly, glycidyl methacrylate (GMA)−iminodiacetic acid (IDA) − $2Na^+$ solution (~17.5 μmol, see Supporting Information for its synthesis) was regulated to pH 7.0 with concentrated hydrochloric acid and then mixed with equimolar

$CuSO_4 \cdot 5H_2O$ in 5 mL of deionized water for 1 h, affording a Cu^{2+} chelating monomer (denoted as GMA − IDA-Cu^{2+}). In this solution, the Lyz-imprinted nanoparticles without template removal (~100mg) were incubated for 1 h for introduction of polymerisable vinyl groups. Next, the resultant nanoparticles after washing with water were re-dispersed in 25 mL of phosphate buffer (pH 7.0, 10 mM) containing MEO_2MA (119.8 mg) and MBA (5.2 mg). After degassed with nitrogen steam for 30 min, this dispersion was mixed with SDS solution (2%, 250 μL) and APS solution (10%, 350 μL) injected sequentially, and then polymerization was continued under magnetic stirring at 37 °C for 12 h. After polymerization, the resultant nanoparticles coated with crosslinked $PMEO_2MA$ layers were washed with EDTA-$2Na^+$ solution (0.1 M) to desorb Cu^{2+}. Finally, the embedded templates were removed in the same way as described above for the Lyz-MIP nanoparticles. The as-prepared imprinted and non-imprinted nanoparticles grafted with crosslinked $PMEO_2MA$ layers are denoted as Lyz-MIP-$PMEO_2MA$ and NIP-$PMEO_2MA$, respectively.

2.4 Protein binding experiments

Protein binding tests for the imprinted and non-imprinted nanoparticles were performed at 25 °C unless otherwise stated. All protein solutions were prepared with phosphate buffer (pH 7.0, 10 mM). The protein binding amount to the nanoparticles at the end of each incubation run was calculated from the following equation:

$$q = (C_0 - C_f)\, V / m \quad (1)$$

where q (mg/g) is the mass of protein adsorbed by unit mass of dry particles, C_0 (mg/mL) and C_f (mg/mL) are the protein concentrations of the initial and final solutions, respectively, V

(mL) is the total volume of the adsorption mixture, and *m* is the mass of the particles used. In each binding run, *V* = 1.5 mL, *m* = ~3 mg. All the tests were conducted in triplicates.

The imprinting effect of a MIP is often evaluated in terms of its imprinting factor (*IF*) and specific binding capacity (*SB*), with the former defined as the ratio of binding capacity of the MIP with respect to that of the NIP and the latter defined as the corresponding difference, i. e.

$$IF = q_{MIP} / q_{NIP} \quad (2)$$

$$SB = q_{MIP} - q_{NIP} \quad (3)$$

where q_{MIP} and q_{NIP} represent the adsorption capacities for the template protein or non-template protein on MIPs and NIPs, respectively.

2.5 SDS-PAGE analysis of Real samples

As a practical sample, chicken egg white separated from a fresh egg was diluted 20-fold with phosphate buffer (pH 7.0, 10 mM) and then centrifuged at 12,000 rpm for 10 min. The resulting supernatant was used as a Lyz source. The nanoparticles (4 mg) were incubated in the supernatant (1.5 mL) for 1 h at room temperature. The nanoparticles were collected and then washed three times with the buffer (1.5 mL). Afterwards, the protein adsorbed to the nanoparticles was eluted using 1% SDS/3% HAc solution (1.5 mL) for 30 min. Finally, the diluted Lyz supernatants before and after adsorption, and the eluents were analyzed by SDS-PAGE with 5% stacking gel and 15% running gel.

2.6. Characterization

The morphologies and structures of the nanoparticles were observed with a transmission

electronic microscopy (TEM) (Tecnai G2 F20, FEI). Zeta potentials were measured using dynamic light scattering (DLS) with a NanoBrook Omni (Brookhaven) laser light scattering spectrometer at the wavelength of 659 nm at 90° angle. Thermogravimetric analysis (TGA) was performed by a NETZSCH TG 209 thermogravimetric analyzer under nitrogen atmosphere with a heating rate of 10 ºC/min up to 800 °C. Fourier-transformation infrared (FT-IR) spectra were determined on a Bio-Rad FTS 135 FT-IR spectrometer over KBr pellets. For the measurement of the thermo-responsiveness of the nanoparticles, the transmittance of their dispersion (0.5 mg/mL) in phosphate buffer (pH 7.0, 10 mM) was monitored as a function of temperature at a wavelength of 600 nm using an UV−vis spectrophotometer (TU-1900, Purkinje General Instrument Co., Beijing) equipped with a temperature controller.

3. Results and discussion

3.1 Synthesis and characterization of Lyz-MIP-PMEO$_2$MA nanoparticles

Our method for the grafting of crosslinked PMEO$_2$MA layers over protein-imprinted PDA coatings is schematically illustrated in Scheme. 1, with Lyz as a model protein template and the SiO$_2$-COOH nanoparticles as representative substrate nanomaterials. The carboxylic groups introduced can capture Lyz from the DA solution before polymerization, hence enhance its imprinting in the resultant PDA coatings [9,25]. The further modification of the core-shell Lyz-MIP nanoparticles was carried out before template removal for protection of the imprints already created. Onto the imprinted PDA coatings, polymerisable vinyl groups were introduced via metal coordination between the amine-containing groups and GMA−IDA −Cu^{2+}. Then, from the PDA coatings bearing vinyl groups, thermo-responsive crosslinked

$PMEO_2MA$ layers were grafted by aqueous precipitation polymerization above the volume phase transition temperature (VPTT) of the resulting $PMEO_2MA$ layers. Finally, template removal was carried out at 4 °C (below the VPTT), so that the $PMEO_2MA$ layers were swollen, hence facilitating the elution of the template.

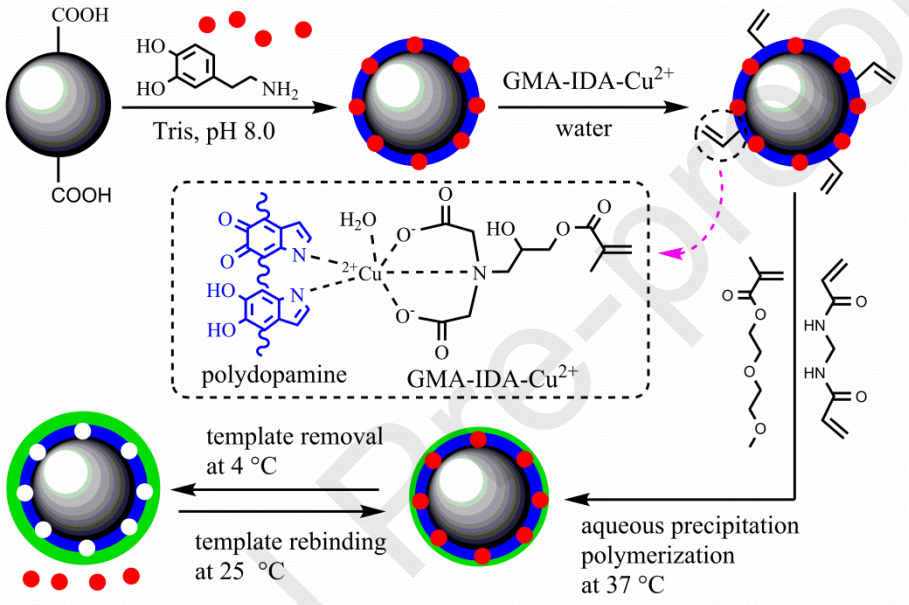

Scheme 1. Schematic diagram for the formation of protein-imprinted polydopamine coatings over carboxyl-functionalized SiO_2 nanoparticles and subsequent modification with thermo-responsive crosslinked $PMEO_2MA$ layers.

Surface imprinting of Lyz as well as other proteins over different support materials based on DA self-polymerization has been extensively studied, including optimization of the thickness of the PDA layers via reaction time or dopamine concentration, and the approaches for eluting protein templates [21,22]. Based on molecular dynamics simulations, it is shown that DA can bind to Lyz via multiple interactions, including hydrogen bonding, π-π stacking,

cation-π interactions and electrostatic interactions (see Fig. S1 in Supporting Information), and these interactions constitute the basis for successful creation of selective recognition nanocavities within the resultant Lyz-imprinted PDA coatings. Herein, the formation of Lyz-imprinted PDA coatings over the SiO_2-COOH nanoparticles was performed according to the previous studies [25] without in-depth investigation, since this work is mainly focused on the post-imprinting modification of the resultant core-shell Lyz-MIP nanoparticles. The grafting of crosslinked $PMEO_2MA$ layers from the vinyl-modified core-shell Lyz-MIP nanoparticles was carried out by aqueous precipitation copolymerization of MEO_2MA with MBA using a fixed total monomer concentration of 0.5 wt% according to our previous studies [47,48].The molar fraction of the crosslinker (MBA) relative to the total monomers, i.e., feed crosslinking degree, was optimized in this work. As shown in Fig. 1, the Lyz-MIP-$PMEO_2MA$ nanoparticles synthesized with a crosslinking degree of 5 mol % showed the highest *IF* value, and thus were employed in the following investigations. Further increasing the feed crosslinking degree may cause the $PMEO_2MA$ layers to be crosslinked excessively, and hence hindering the diffusion of Lyz to the internal imprinting sites.

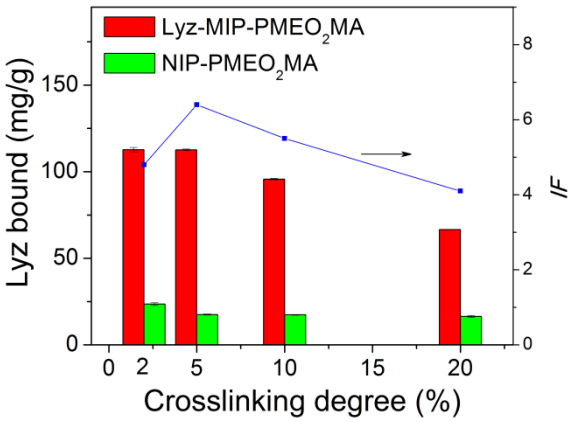

Fig. 1. Effect of the feed crosslinking degrees on Lyz rebinding to the resultant

Lyz-MIP-PMEO$_2$MA and NIP-PMEO$_2$MA nanoparticles. C_0 = 0.4 mg mL^{-1}.

The successful formation of the PDA and PMEO$_2$MA layers on the imprinted nanoparticles was confirmed by the FT-IR spectra (see Fig. S2 in Supporting Information). TEM was employed to observe the morphologies of the different nanoparticles. As shown in Fig. 2, the SiO$_2$−COOH nanoparticles is about 280 nm in diameter. All of the MIP and NIP nanoparticles, whether or not grafted with PMEO$_2$MA, retained uniformly spherical shape like the SiO$_2$−COOH nanocores. The imprinted PDA coatings of the Lyz-MIP nanoparticles can be distinguished from the inside silica cores; whereas the non-imprinted coatings cannot be clearly discriminated from the NIP particles, probably due to the too small thickness. After further grafting of crosslinked PMEO$_2$MA layers, the increase in the thickness of the dual-layer polymer is not remarkable for the imprinted nanoparticles, while the polymer shells still cannot be clearly observed from the non-imprinted particles.

Fortunately, TGA can prove the existence of both the PDA coatings over the SiO$_2$-COOH nanoparticles and the PMEO$_2$MA layers grafted subsequently, for both the imprinted and non-imprinted particles (see Fig. S3 in Supporting Information). According to the TG curves, the Lyz-MIP and NIP shells relative to the SiO$_2$-COOH cores were calculated to be 12.5 wt% and 7.2 wt%, respectively; while the mass percentages of the grafted PMEO$_2$MA layers with respect to the original Lyz-MIP and NIP nanoparticles were estimated to be 4.2 wt% and 3.0 wt%, respectively. It is noted that the mass of the imprinted PDA coatings grafted on the SiO$_2$-COOH nanoparticles is significantly higher than that of the non-imprinted coatings. Such remarkable difference was rarely reported in previous studies on protein-imprinting

PDA coatings, since TGA was usually performed only for the imprinted PDA coatings and the corresponding substrate materials, but not for the non-imprinted controls [25,26,29,34]. However, this result is consistent with that observed from the surface protein imprinting via free radical polymerization [47,48], and can be explained similarly as follows. The positively charged Lyz molecules in the pre-polymerization solution can be adsorbed onto the surface of the negative SiO_2-COOH core particles via electrostatic interactions, and the adsorbed Lyz molecules can increase the local DA concentration around the core particles due to the Lyz−DA interactions, hence promoting the surface polymerization. Therefore, the mass of the Lyz-MIP shells grafted to the core particles is higher than that of the NIP shells formed in the absence of Lyz. Notwithstanding, the above defined *IF* is generally employed to evaluate the imprinting performance of the core-shell protein-imprinted particles, since that the binding to the non-imprinted particles primarily depends on their surface properties. On the other hand, the mass of the $PMEO_2MA$ layers grafted to the core-shell Lyz-MIP nanoparticles is higher than to the NIP nanoparticles. This phenomenon can be explained in the following way. For effective grafting of the $PMEO_2MA$ layers via radical-induced surface polymerization, polymerisable vinyl groups were anchored on the Lyz-MIP or NIP nanoparticles via the metal-coordination between GMA-IDA-Cu^{2+} and the amine-containing groups on the PDA coatings. During this process, some Lyz molecules present near the surface of the Lyz-MIP nanoparticles can also interact with GMA-IDA-Cu^{2+} via coordination. As a result, the Lyz-MIP nanoparticles can bear some more vinyl groups than the NIP controls, and hence were grafted with higher mass of $PMEO_2MA$ layers after the polymerization as shown above.

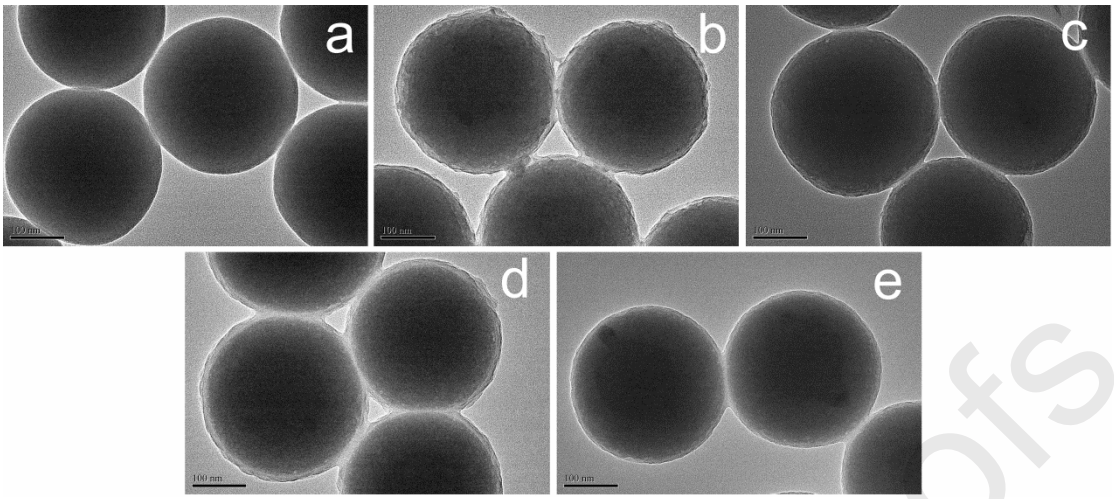

Fig. 2. TEM images of (a) SiO_2-COOH, (b) Lyz-MIP, (c) NIP, (d) Lyz-MIP-$PMEO_2MA$, and (e) NIP-$PMEO_2MA$ nanoparticles. All the scale bars represent 100 nm.

Each step of the functionalization was also monitored by zeta potential measurements. A shown in Fig. 3A, both the Lyz-MIP and NIP nanoparticles show approximately equal zeta potentials, and are significantly less negative than the SiO_2-COOH nanoparticles. Furthermore, their zeta potentials are very close to the values measured previously with PDA coatings [49]. Therefore, these results can further prove the formation of the PDA coatings on both the Lyz-MIP and NIP nanoparticles. After grafted with crosslinked $PMEO_2MA$ layers, both the Lyz-MIP and NIP nanoparticles become only slightly negative charged, because of the charge screening effect of the nonionic $PMEO_2MA$ layers.

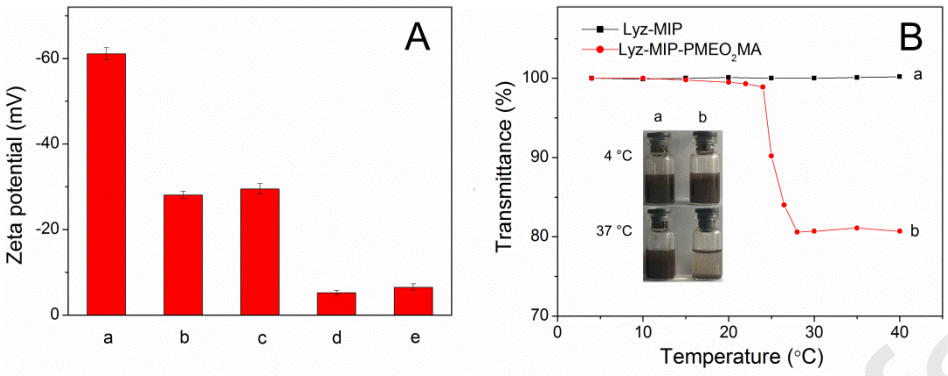

Fig. 3. (A) Zeta potentials of (a) SiO_2-COOH, (b) Lyz-MIP, (c) NIP, (d) Lyz-MIP-$PMEO_2MA$, and (e) NIP-$PMEO_2MA$ nanoparticles measured in phosphate buffer (pH 7.0). (B) Transmittance of aqueous dispersions of (a) Lyz-MIP and (b) Lyz-MIP-$PMEO_2MA$ nanoparticles with increasing temperatures. The insets show the images of these dispersions (0.5 mg/mL) after 1-hour setting at 4 or 37 °C, respectively.

The functionalization with $PMEO_2MA$ also endowed the Lyz-MIP nanoparticles with thermo-responsiveness, which was confirmed by measuring the turbidity of the aqueous dispersion with increasing temperatures. As shown from Fig. 3B, the Lyz-MIP-$PMEO_2MA$ nanoparticles illustrate remarkable temperature-responsive in contrast to the Lyz-MIP controls, with a VPTT of about 25 °C, which is very close to the reported LCST of $PMEO_2MA$ homopolymers (26 °C) [46]. Therefore, the Lyz-MIP-$PMEO_2MA$ nanoparticles tended to settle at 37 °C (above the VPTT) due to the state transformation of the $PMEO_2MA$ layers from hydrophile to hydrophobe, in contrast to the situation at 4 °C (below the VPTT).

3.2 Effect of crosslinked $PMEO_2MA$ layers on protein binding properties

Due to the thermo-responsiveness of the $PMEO_2MA$ layers, Lyz binding was first

investigated at three different temperatures (4, 25 and 37 °C) (see Fig. S4 in Supporting Information). The Lyz-MIP-PMEO$_2$MA nanoparticles demonstrate approximate *IF* and *SB* at both 25 and 37 °C, whereas with significantly lower *SB* at 4 °C. Therefore, the following binding tests were performed at 25 °C, considering that the Lyz-MIP-PMEO$_2$MA nanoparticles showed better aqueous dispersion at 25 °C than at 37 °C.

For proving the efficacy of the grafted PMEO$_2$MA layers in increasing protein binding selectivity, single-protein batch adsorption tests were performed using four reference proteins with a wide range of isoelectric point (pI) and molecular weight (Mw) for comparison with Lyz. All the proteins used are Lyz (Mw 14 k, pI 11.1), cytochrome c (Cyt c, Mw 12.4 k, pI 10.2), ribonuclease A (RNase A, Mw 13.7 k, pI 9.6), BHb (Mw 64.5 k, pI 6.8), and bovine serum albumin (BSA, Mw 66 k, pI 4.8). Fig 4a shows the binding capacities of the imprinted and non-imprinted particles for these proteins at 25 °C with a feed concentration of 0.4 mg mL^{-1}. The Lyz-MIP nanoparticles before PMEO$_2$MA modification show notably selectivity for Lyz, with an *IF* of 2.6, at least twice larger than the *IF* values for other control proteins, in agreement with the result reported previously [25]. After grafted with the protein-resistant PMEO$_2$MA layers, both the imprinted and non-imprinted particles show some reduction in binding of all the proteins studied. However, the decrease extent in Lyz binding to the Lyz-MIP-PMEO$_2$MA particles is significantly lower because of the high-affinity cavities inside for Lyz. Therefore, after the grafting of PMEO$_2$MA layers, the *IF* of the imprinted nanoparticles for Lyz increased from 2.6 to 6.4, while the *IF* values for other proteins showed only little change. It should be noted that this *IF* up to 6.4 is also much higher than achieved with the PDA based Lyz-imprinted materials reported previously (See Table S1 in Supporting

Information). On the other hand, the Lyz-MIP-PMEO$_2$MA nanoparticles exhibit even slightly higher *SB* for Lyz than the Lyz-MIP particles, increasing from 87.4 to 93.2 mg/g. Furthermore, such protein binding selectivity enhancement by modification with PMEO$_2$MA layers was also verified by the binary protein competitive adsorption experiments with Cyt c as the competitor, as shown from Fig. 4b.

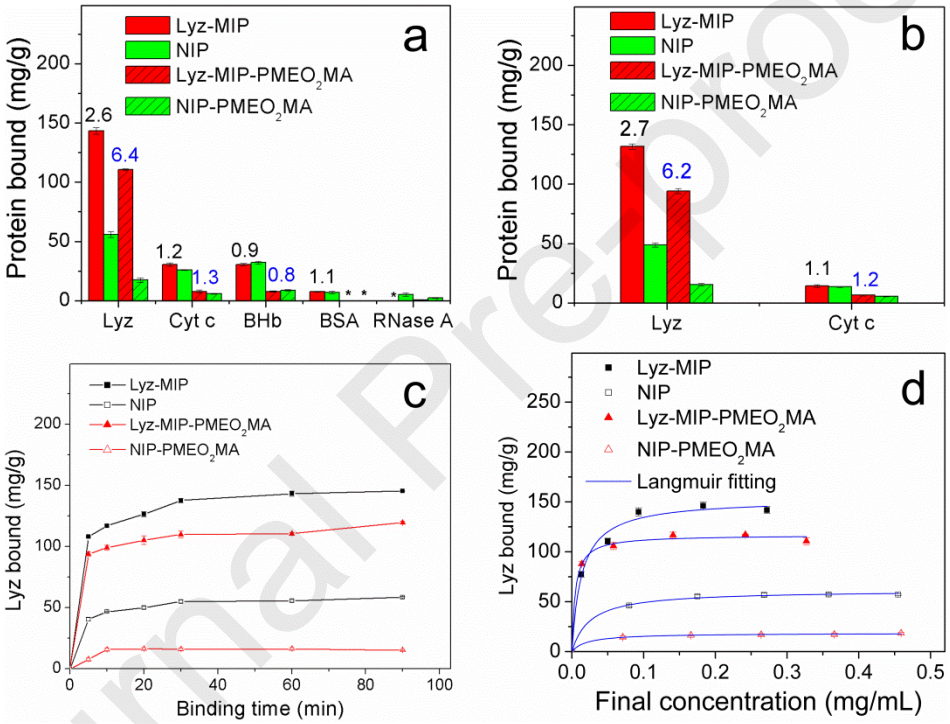

Fig.4. Protein binding properties to the Lyz-imprinted and non-imprinted nanoparticles with or without grafting of PMEO$_2$MA layers: (a) binding of Lyz and other four kinds of control proteins (C_0 = 0.4 mg mL^{-1}); (b) competitive binding of Lyz and Cyt c, $C_{0,\mathrm{Lyz}} = C_{0,\mathrm{Cyt\,c}}$ = 0.2 mg mL^{-1}; (c) Lyz binding kinetics profiles (C_0 = 0.4 mg mL^{-1}); (d) Lyz binding isotherms. The imprinting factors are indicated above the bars. * Denotes too little to be detected.

As the first and only study on post-imprinting modification of protein-imprinted PDA

coatings reported before, Li et al. [41] grafted PMPC chains from the PDA-based core-shell BSA-imprinted magnetic microspheres by surface-initiated ATRP of MPC. The zwitterionic PMPC chains grafted with the optimized ATRP condition resulted in *IF* increase from 1.5 to 5.7, along with *SB* increase from 3.3 to 6.8 mg/g. Obviously, this approach showed remarkable efficacy in reduction of nonspecific binding. However, it is difficult to directly compare this approach with our method in selectivity enhancement, since that the two studies employed different protein templates, also the core-shell BSA-imprinted microspheres before ATRP modification showed quite low BSA binding capacity (~9.4 mg/g), remarkable lower than the corresponding Lyz binding capacity (143.2 mg/g). Nevertheless, the noticeable advantage of our method lies in the facile radical polymerization with green and mild reaction condition (aqueous, 37 °C), while the ATRP method was not easily performed (especially at up to 80 °C), and also required use of organic reaction solvents (CH_2Cl_2 and DMF).

The recognition selectivity of the Lyz-MIP and Lyz-MIP-PMEO_2MA nanoparticles were further compared by selective capture of Lyz from a real sample, i.e. 20-fold diluted egg white solution. The SDS-PAGE analyses for the samples after different treatments were shown in Fig. S5 in Supporting Information. Most remarkably, only a single band corresponding to Lyz appears in the lane 8 for the eluent from the Lyz-MIP-PMEO_2MA nanoparticles; while in lane 6 for the eluent from the Lyz-MIP nanoparticles, another band (corresponding to ovalbumin) is present besides the Lyz band. This result further confirmed that introduction of the PMEO_2MA layers over the Lyz-imprinted PDA coatings can improve their recognition selectivity.

The binding kinetics to the two kinds of imprinted and non-imprinted nanoparticles was

investigated with an initial Lyz concentration of 0.4 mg mL^{-1}. As shown from Fig. 4c, all the adsorbents reached saturated binding within 30 min, and this binding rate is comparable to that reported previously with the protein-imprinted PDA coatings [25,27,29]. This means that the slightly crosslinked $PMEO_2MA$ layers grafted outsides the imprinted PDA coatings showed no significant hindrance to protein diffusion to the imprints beneath.

The binding equilibriums to the imprinted and non-imprinted nanoparticles were studied at different initial Lyz concentrations ranging from 0.1 to 1.0 mg mL^{-1}. Fig. 4d shows the binding isotherms at different equilibrium concentrations. The Langmuir model was used to describe the experimental data, which is expressed as

$$q_e = q_m \cdot C_e / (K_d + C_e) \quad (4)$$

where C_e (mg mL^{-1}) is the equilibrium concentration of Lyz in bulk solution, q_e (mg g^{-1}) the amount of bound Lyz on per gram of the adsorbents at the equilibrium concentration, q_m (mg g^{-1}) the saturation capacity and K_d (mg mL^{-1}) the dissociate constant. Nonlinear fitting of the experimental data to the Langmuir equation led to a good fit for all the adsorbents, hence allowing for determining the involved parameters. The estimated values of q_m and K_d, for the two kinds of imprinted and non-imprinted nanoparticles are listed in Table S2 in Supporting Information. Also, the *IF* and *SB* were calculated based on the estimated q_m, respectively. It can be seen that, the grafting of the $PMEO_2MA$ layers led to *IF* increase from 2.6 to 6.3 and *SB* increase from 96.3 to 98.2 mg g^{-1}. Notably, the K_d for the Lyz-MIP-$PMEO_2MA$ nanoparticles are significantly lower than for Lyz-MIP controls, suggesting some increase in affinity due to the $PMEO_2MA$ modification. This may be explained in this way. The formation of the crosslinked $PMEO_2MA$ layers in the presence of the template may further

enhance imprinting of the template molecules approaching the surface of the imprinted PDA coatings.

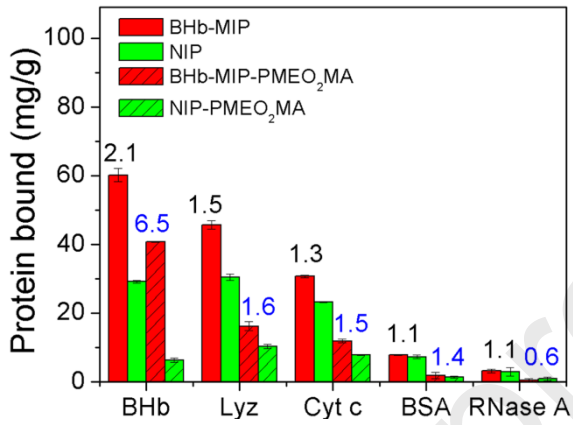

Fig. 5. Binding selectivity of the BHb-imprinted or non-imprinted nanoparticles with or without grafting of crosslinked $PMEO_2MA$ layers (C_0 = 0.4 mg mL^{-1}). The imprinting factors are indicated above the bars.

3.3. Preliminary extension to imprinting of BHb

To test the generality of the strategy presented in this work, we chose BHb as another protein template for a preliminary investigation. The BHb-imprinted PDA coatings on the surface of SiO_2 nanoparticles were prepared according to a previous study [23]. Pristine SiO_2 nanoparticles without any modification were directly used as the nano-substrates, since BHb can form strong interactions with the surface Si-OH groups. The crosslinked $PMEO_2MA$ layers were grafted outside the core-shell BHb-imprinted nanoparticles by the same way as imprinting of Lyz. As can be seen from Fig. 5, the $PMEO_2MA$ modified BHb-imprinted nanoparticles also show remarkably increased recognition selectivity for BHb in comparison

to the unmodified controls, with *IF* increasing from 2.1 to 6.5 and *SB* increasing from 31.0 to 34.5 mg/g. However, the $PMEO_2MA$ modification brought about much slighter *IF* change for the reference proteins.

3.4. Influence of crosslinked $PMEO_2MA$ layers on stability of imprinted PDA coatings

The stability of PDA coatings has attracted some attention in the areas of materials and chemistry. Previous studies proved that the PDA coatings show some detachment from the substrate materials under acidic or basic conditions, and the stability is dependent on the pH of aqueous solutions, the nature of the used substrate as well as the deposition method used [49-51]. The acidic SDS/HAc solution is widely employed for template removal from protein-imprinted PDA coatings. Therefore, the repeated use of the imprinted nanoparticles were examined by removal of the adsorbed template protein with the 1% SDS/3% HAc solution by the same as they were synthesized, and then the regenerated nanoparticles were reused to bind the template protein. As shown in Fig. 6, before grafting of the $PMEO_2MA$ layers, Lyz binding to the Lyz-MIP nanoparticles shows only slight decrease after three adsorption-regeneration cycles. However, BHb binding to the BHb-MIP nanoparticles exhibits great reduction even at the second binding test. Moreover, noticeable PDA detachment was observed from the BHb-MIP nanoparticles while regenerated with the SDS/HAc solution. This may be explained as follows. While surface imprinting of Lyz or BHb at pH 8.0, larger amount of Lyz (pI 11.1, positively charged) could be adsorbed onto the oppositely charged SiO_2-COOH nanoparticles than BHb (pI 6.8, negatively charged) onto the likely charged SiO_2 nanoparticles, and the more protein molecules adsorbed on the

surface of the nano-substrates may contribute to the formation of the more stable protein-imprinted PDA coatings. This result is consistent with previous finding that the surface chemistry of substrate materials can affect the chemical stability of the PDA coatings [49-51]. Nonetheless, after coated with the $PMEO_2MA$ layers, either Lyz or BHb imprinted nanoparticles demonstrates almost no significant reduction in template binding after three adsorption-regeneration cycles. Therefore, the $PMEO_2MA$ layers can enhance the stability of protein-imprinted PDA coatings.

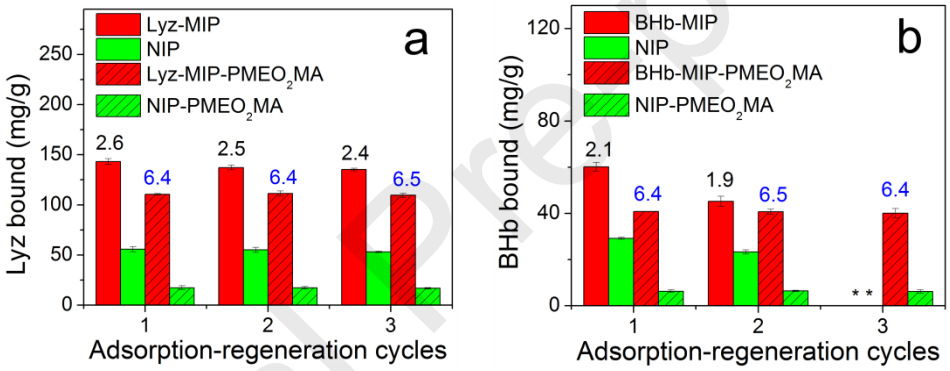

Fig. 6. Influence of the regeneration cycles on protein binding to the imprinted or non-imprinted nanoparticles with or without grafting of crosslinked $PMEO_2MA$ layers (regenerated by washing with 1% SDS/3% HAc solution at 4 °C; C_0 = 0.4 mg mL^{-1}): (a) Lyz-imprinted nanoparticles; (b) BHb-imprinted nanoparticles. The imprinting factors are indicated above the bars. * Most of the PDA coatings were detached and hence the adsorption was not carried out.

4. Conclusions

In summary, we have demonstrated a facile method for reducing non-specific binding to

the protein-imprinted PDA coatings, with SiO_2 nanoparticles as representative substrate materials and Lyz and BHb as model templates. Through aqueous precipitation polymerization, cross-linked $PMEO_2MA$ layers were successfully grafted onto the core-shell imprinted nanoparticles after introduction of vinyl groups via Cu^{2+} mediated metal coordination. The cross-linked $PMEO_2MA$ layers grafted could significantly increase the recognition selectivity and specific binding to the imprinted nanoparticles, and could also enhance the stability of the imprinted PDA coatings in the acidic conditions for template removal. The method presented may be readily generalized to the other molecularly imprinted PDA coatings with other substrate materials and other bio/organic molecules as templates.

Acknowledgements

This work was supported by the National Natural Science Foundation of China (No. 21544006, 21674051 and 81771986), the Natural Science Foundation of Tianjin City (No. 15JCYBJC47400), and the National Key R&D Program of China (2017YFC11044001).

Appendix A. Supplementary material

Supplementary data associated with this article can be found in the on line version at

References

[1] L.X Chen, S.F.Xu, J.H.Li, Recent advances in molecular imprinting technology: current status, challenges and highlighted applications, Chem. Soc. Rev. 40 (2011) 2922–2942.

[2] D.R.Kryscio, N.A.Peppas, Critical review and perspective of macromolecularly imprinted

polymers, Acta Biomater. 8 (2012) 461–473.

[3] S.J Li, S.S. Cao, M.J. Whitcombe, S.A. Piletsky, Size matters: challenges in imprinting macromolecules, Prog. Polym. Sci. 39 (2013) 145–163.

[4] M. Dabrowski, P. Lach, M. Cieplak, W. Kutner, Nanostructured molecularly imprinted polymers for protein chemosensing, Biosens. Bioelectron. 102 (2018) 17–26.

[5] H. Nishino, C.S. Huang, K.J. Shea, Selective protein capture by epitope imprinting, Angew. Chem. Int. Ed. 45 (2006) 2392–2396.

[6] X.T. Shen, T.C. Zhou, L. Ye, Molecular imprinting of protein in pickering emulsion, Chem. Commun. 48 (2012) 8198–8200.

[7] A. Nematollahzadeh, W. Sun, C.S.A. Aureliano, D. Lutkemeyer, J. Stute, M.J. Abdekhodaie, A. Shojaei, B. Sellergren, High-capacity hierarchically imprinted polymer beads for protein recognition and capture, Angew. Chem. Int. Ed. 50 (2011) 495–498.

[8] T. Shiomi, M. Matsui, F. Mizukami, K. Sakaguchi, A method for the molecular imprinting of hemoglobin on silica surface susing silanes, Biomaterials 26 (2005) 5564–5571.

[9] G.Q. Fu, H.Y. He, Z.H. Chai, H.C. Chen, J. Kong, Y. Wang, Y.Z. Jiang, Enhanced lysozyme imprinting over nanoparticles functionalized with carboxyl groups for noncovalent template sorption, Anal. Chem. 83 (2011) 1431–1436.

[10] X.J. Li, B.L. Zhang, W. Li, X.F. Lei, X.L. Fan, L. Tian, H.P. Zhang, Q.Y. Zhang, Preparation and characterization of bovine serum albumin surface-imprinted thermosensitive magnetic polymer microsphere and its application for protein recognition, Biosens. Bioelectron. 51 (2014) 261–267.

[11] A. Abbas, L.M. Tian, J.J. Morrissey, E.D. Kharasch, S. Singamaneni, Hot spot-localized

artificial antibodies for label-free plasmonic biosensing, Adv. Funct. Mater. 23 (2013) 1789–1797.

[12] R. Hu, J.Y. Luan, E.D. Kharasch, S. Singamaneni, J. J. Morrissey, Aromatic functionality of target proteins influences monomer selection for creating artificial antibodies on plasmonic biosensors, ACS Appl. Mater. Interfaces 9 (2017) 245−251.

[13] S. Ambrosini, S. Beyazit, K. Haupt, B.T.S. Bui, Solid-phase synthesis of molecularly imprinted nanoparticles for protein recognition, Chem. Commun. 49 (2013) 6746–6748.

[14] Y. Hoshino, T. Kodama, Y. Okahata, K.J. Shea, Peptide imprinted polymer nanoparticles: a plastic antibody, J. Am. Chem. Soc. 130 (2008) 15242–15243.

[15] A. Cutivet, C. Schembri, J. Kovensky, K. Haupt, Molecularly imprinted microgels as enzyme inhibitors, J. Am. Chem. Soc. 131 (2009) 14699–14702.

[16] G.Q. Pan, Q.P. Guo, C.B. Cao, H.L. B. Yang, Li, Thermo-responsive molecularly imprinted nanogels for specific recognition and controlled release of proteins, Soft Matter 9 (2013) 3840–3850.

[17] Y.Q. Lv, T.W. Tan, F. Svec, Molecular imprinting of proteins in polymers attached to the surface of nanomaterials for selective recognition of biomacromolecules, Biotechnol. Adv. 31 (2013) 1172–1186.

[18] H. Lee, S.M. Dellatore, W.M. Miller, P.B. Messersmith, Mussel-inspired surface chemistry for multifunctional coatings, Science 318 (2007) 426–430.

[19] R.Z. Ouyang, J.P. Lei, H.X. Ju, Surface molecularly imprinted nanowire for protein specific recognition, Chem. Comm. 44 (2008), 5761–5763.

[20] Y.L. Liu, K.L. Ai, L.H. Lu, Polydopamine and its derivative materials: synthesis and

promising applications in energy, environmental, and biomedical fields, Chem. Rev. 114 (2014), 5057−5115.

[21] S. A. Zaidi, An account on the versatility of dopamine as a functional monomer in molecular imprinting, ChemistrySelect 4 (2019), 5081–5090.

[22] M.Y. Li, M.H. Zhao, J.Q. Zhai, M.P. Zhao, Dopamine-based molecularly imprinted polymers for the recognition of biomacromolecules, Chin. Sci. Bull. 64 (2019) 1321–1329.

[23] Z.W. Xia, Z.A. Lin, Y. Xiao, L. Wang, J.N. Zheng, H.H. Yang, G.N. Chen, Facile synthesis of polydopamine-coated molecularly imprinted silica nanoparticles for protein recognition and separation, Biosens. Bioelectron. 47 (2013) 120–126.

[24] W.H. Zhou, C.H. Lu, X.C. Guo, F.R. Chen, H.H. Yang, X.R. Wang, Mussel-inspired molecularly imprinted polymer coating superparamagnetic nanoparticles for protein recognition, J. Mater. Chem. 20 (2010) 880–883.

[25] M. Zhang, X.H. Zhang, X.W. He, L.X. Chen, Y.K. Zhang, A self-assembled polydopamine film on the surface of magnetic nanoparticles for specific capture of protein, Nanoscale 4 (2012) 3141–3147.

[26] R.X. Gao, L.L. Zhang, Y. Hao, X.H. Cui, Y.H. Tang, Specific removal of protein using protein imprinted polydopamine shells on modified amino-functionalized magnetic nanoparticles, RSC Adv. 4 (2014) 64514–64524.

[27] R.Z. Ouyang, J.P. Lei, H.X. Ju, Artificial receptor-functionalized nanoshell: facile preparation, fast separation and specific protein recognition, Nanotechnology 21 (2010) 185502.

[28] J.Q. Zhai, M.H. Zhao, X.J. Cao, M.Y. Li, M.P. Zhao, Metal-ion-responsive

bionanocomposite for selective and reversible enzyme inhibition, J. Am. Chem. Soc. 140 (2018) 16925–16928.

[29] X.P. Jia, M.L. Xu, Y.Z. Wang, D. Ran, S. Yang, M. Zhang, Polydopamine-based molecular imprinting on silica-modified magnetic nanoparticles for recognition and separation of bovine hemoglobin, Analyst 138 (2013) 651–658.

[30] S.W. Li, K.K. Yang, J.X. Liu, B. Jiang, L.H. Zhang, Y.K. Zhang, Surface-imprinted nanoparticles prepared with a his-tag-anchored epitope as the template, Anal. Chem. 87 (2015) 4617–4620.

[31] X.Y. Wang, J.L. Yu, J.H. Li, Q. Kang, D.Z. Shen, L.X. Chen, Quantum dots based imprinting fluorescent nanosensor for the selective and sensitive detection of phycocyanin: a general imprinting strategy toward proteins, Sens. Actuators, B. 255 (2018) 268–274.

[32] T. Chen, M.W. Shao, H.Y. Xu, S.J. Zhuo, S.S. Liu, S.T. Lee, Molecularly imprinted polymer-coated silicon nanowires for protein specific recognition and fast separation, J. Mater. Chem. 22 (2012) 3990–3996.

[33] C. Zheng, X.L. Zhang, W. Liu, B. Liu, H.H. Yang, Z.A. Lin, G.N. Chen, A selective artificial enzyme inhibitor based on nanoparticle-enzyme interactions and molecular imprinting, Adv. Mater. 25 (2013) 5922–5927.

[34] J. Luo, S.S. Jiang, X.Y. Liu, Efficient one-pot synthesis of mussel-inspired molecularly imprinted polymer coated graphene for protein-specific recognition and fast separation, J. Phys. Chem. C 736 (2013) 18448–18456.

[35] A. Tretjakov, V. Syritski, J. Reut, R. Boroznjak, O. Volobujeva, A. Öpik, Surface molecularly imprinted polydopamine films for recognition of immunoglobulin G, Microchim.

Acta 180 (2013) 1433–1442.

[36] C.H. Lu, Y. Zhang, S.F. Tang, Z.B. Fang, H.H. Yang, X. Chen, G.N. Chen, Sensing HIV related protein using epitope imprinted hydrophilic polymer coated quartz crystal microbalance, Biosens. Bioelectron. 31(2012) 439–444.

[37] A. Nematollahzadeh, A. Shojaei, M.J. Abdekhodaie, B. Sellergren, Molecularly imprinted polydopamine nano-layer on the pore surface of porous particles for protein capture in HPLC column, J. Colloid Interface Sci. 404 (2013) 117–126.

[38] J.H. Ryu, P.B. Messersmith, H. Lee, Polydopamine surface chemistry: a decade of discovery, ACS Appl. Mater. Interfaces 10 (2018) 7523–7540.

[39] Y.L. Liu, K.L. Ai, L.H. Lu, Polydopamine and its derivative materials: synthesis and promising applications in energy, environmental, and biomedical fields, Chem. Rev. 114 (2014) 5057–5115.

[40] H. Lee, J. Rho, P.B. Messersmith, Facile conjugation of biomolecules onto surfaces via mussel adhesive protein inspired coatings, Adv. Mater. 20 (2008) 1–4.

[41] X.J. Li, J.J. Zhou, L. Tian, Y.F. Wang, B.L. Zhang, H.P. Zhang, Q.Y. Zhang, Preparation of anti-nonspecific adsorption polydopamine-based surface protein-imprinted magnetic microspheres with the assistance of 2-methacryloyloxyethyl phosphorylcholine and Its application for protein recognition, Sens. Actuators, B 241 (2017) 413–421.

[42] J.Y. Luan, K.K. Liu, S. Tadepalli, Q.S. Jiang, J.J. Morrissey, E.D. Kharasch, S. Singamaneni, PEGylated artificial antibodies: plasmonic biosensors with improved selectivity, ACS Appl. Mater. Interfaces 8 (2016), 23509−23516.

[43] X. Qian, X.H. Peng, D.O. Ansari, Q. Yin-Goen, G.Z. Chen, D.M. Shin, L. Yang, A.N.

Young, M.D. Wang, S. Nie, In vivo tumor targeting and spectroscopic detection with surface-enhanced raman nanoparticle tags, Nat. Biotechnol. 26 (2007), 83−90.

[44] L. Cheng, C. Wang L., Feng, K. Yang, Z. Liu, Functional nanomaterials for phototherapies of cancer, Chem. Rev. 114 (2014) 10869−10939.

[45] T. Pochechueva, A.Chinarev, N. Bovin, A. Fedier, F. Jacob, V. Heinzelmann-Schwarz, PEGylation of microbead surfaces reduces unspecific antibody binding in glycan-based suspension array, J. Immunol. Methods 412 (2014) 42−52.

[46] J.F. Lutz, Polymerization of oligo(ethylene glycol) (meth)acrylates: toward new generations of smart biocompatible materials, J. Polym. Sci., Part A: Polym. Chem. 46 (2008) 3459–3470.

[47] C.C. Yang, X.M. Yan, H. Guo, G.Q. Fu, Synthesis of surface protein-imprinted nanoparticles endowed with reversible physical cross-links, Biosens. Bioelectron. 75 (2016) 129–135.

[48] W. Li, Y. Sun, C.C. Yang, X.M. Yan, H. Guo, G.Q. Fu, Fabrication of surface protein-imprinted nanoparticles using a metal chelating monomer via aqueous precipitation polymerization, ACS Appl. Mater. Interfaces 7 (2015) 27188–27196.

[49] H.L. Wei, J. Ren, B. Han, L. Xu, L.L. Han, L.Y. Jia, Stability of polydopamine and poly(DOPA) melanin-like films on thesurface of polymer membranes under strongly acidic and alkalineconditions, Colloids Surf., B 110 (2013) 22– 28.

[50] W.C. Yang, J. Liu, Y. Chen, Stability of polydopamine coatings on gold substrates inspected by surface plasmon resonance imaging, Langmuir 34 (2018) 3565−3571.

[51] C. Zhang, Y. Ou, W.X. Lei, L.S. Wan, J. Ji, Z.K. Xu, $CuSO_4/H_2O_2$-induced rapid

deposition of polydopamine coatings with high uniformity and enhanced stability, Angew. Chem. Int. Ed. 55 (2016) 3054–3057.

Declaration of interests

☐ v The authors declare that they have no known competing financial interests or personal relationships that could have appeared to influence the work reported in this paper.

☐The authors declare the following financial interests/personal relationships which may be considered as potential competing interests:

Highlights

- Protein- resistant layers were grafted to protein-imprinted polydopamine coatings
- Great increase in the imprinting factor of the imprinted polymers
- No decrease in the specific binding capacity of the imprinted polymers
- Significant improvement of the stability of the imprinted polymers in acidic media